

## Rectification of acetylcholine-elicited currents in PC12 pheochromocytoma cells

(neuronal nicotinic acetylcholine receptor/current–voltage relationship/magnesium block)

C. K. IFUNE\* AND J. H. STEINBACH†

\*Neural Science Program, Division of Biomedical Sciences; and †Departments of Anesthesiology and of Anatomy and Neurobiology, Washington University School of Medicine, Saint Louis, MO 63110

Communicated by G. D. Fischbach, March 29, 1990

**ABSTRACT** The current–voltage ( $I$ – $V$ ) relationship for acetylcholine-elicited currents in the rat pheochromocytoma cell line PC12 is nonlinear. Two voltage-dependent processes that could account for the whole-cell current rectification were examined, receptor channel gating and single receptor channel permeation. We found that both factors are involved in the rectification of the whole-cell currents. The voltage dependence of channel gating determines the shape of the  $I$ – $V$  curve at negative potentials. The single-channel  $I$ – $V$  relationship is inwardly rectifying and largely responsible for the characteristic shape of the whole-cell  $I$ – $V$  curve at positive potentials. The rectification of the single-channel currents is produced by the voltage-dependent block of outward currents by intracellular  $Mg^{2+}$  ions.

Inward rectification of acetylcholine (ACh)-elicited currents is a common feature of ganglion cells of the mammalian peripheral nervous system. Nonlinear current–voltage ( $I$ – $V$ ) relationships have been described for excitatory synaptic currents in rabbit superior cervical ganglion (SCG) cells (1) and mouse submandibular ganglion cells (2). Inwardly rectifying ACh-elicited currents have been seen in rat sympathetic ganglion cells (3, 4), rat and mouse parasympathetic ganglion cells (L. Fieber and D. Adams, personal communication; ref. 2), rat adrenal chromaffin cells (5), and rat SCG cells (6). The inward rectification of the ACh-elicited currents in these cells apparently results from different mechanisms. The voltage dependence of channel opening appears to be responsible for the rectification in rat sympathetic ganglion cells (4). For rat SCG cells, Selyanko *et al.* (6) have concluded that the rectification can be completely explained by the voltage dependence of the channel open time determined from ACh-receptor current relaxations after voltage jumps. The mechanism responsible for rectification of the ACh-elicited current in rat adrenal chromaffin cells has not been thoroughly studied, although Hirano *et al.* (5) have speculated that the rectification they observed might have been due to voltage-dependent block by intracellular  $Cs^+$ . In mouse submandibular ganglion cells, the shape of the whole-cell  $I$ – $V$  relationship has been attributed to the voltage dependence of the probability of a channel being open and the nonlinearity of the single-channel conductance (2).

Cells of the PC12 clonal cell line, derived from a rat pheochromocytoma (7), differentiate into sympathetic neuron-like cells in response to nerve growth factor; the differentiated PC12 cells express nicotinic ACh receptors (8) similar to those found on sympathetic neurons (9, 10). The  $I$ – $V$  relationship for the whole-cell ACh-elicited current in PC12 cells greatly resembles that found for rat chromaffin (5) and rat SCG (6) cells. Here we show that the rectification of the macroscopic ACh-receptor current in PC12 cells cannot

be entirely explained by the voltage dependence of channel gating. Rather, the single-channel  $I$ – $V$  relationship determined by the intracellular  $Mg^{2+}$  concentration dominates the  $I$ – $V$  relationship of the whole-cell current.

### MATERIALS AND METHODS

**Tissue Culture.** The PC12H cell line was kindly provided by D. Schubert (Salk Institute). Cells were grown (11) in Dulbecco's modified Eagle's medium containing 10% heat-inactivated fetal bovine serum and 5% heat-inactivated horse serum (Hazelton Research Products, Lenexa, KS) and were passaged weekly. For patch-clamp experiments, cells were plated onto collagen-coated 35-mm plastic tissue culture dishes (Vitrogen 100, Collagen Corp.), and treated with 4 nM (100 ng/ml) mouse  $\beta$  nerve growth factor (provided by E. Johnson, Washington University School of Medicine). Cultures were fed three times a week and used 5–10 days after plating.

**Physiological Recordings.** Recordings were obtained using the List EPC-7 patch clamp. Records from whole-cell and outside-out patches (12) were acquired using the PCLAMP programs (Axon Instruments, Foster City, CA) and a 386 Zenith personal computer. Data were analyzed using BINFITS (C. Lingle, Washington University School of Medicine). Pipettes were pulled from KG33 borosilicate capillaries by using a P-80/PC micropipette puller (Sutter Instrument, San Rafael, CA) and coated with Sylgard 182 (Dow). After fire-polishing, pipette resistances were 2–5 M $\Omega$  when the pipettes were filled with sodium isethionate intracellular solution (see below). For whole-cell recordings, the EPC-7 circuitry was used to cancel the capacity charging transients and to compensate for the series resistance, which ranged from 5 to 30 M $\Omega$ . Series resistances were 70–80% compensated. Whole-cell and single-channel records were filtered at 2 kHz with an eight-pole low-pass Bessel filter. All experiments were conducted at room temperature (18–19°C) unless specified otherwise.

Whole-cell  $I$ – $V$  relationships were determined from peak currents elicited by ACh application to cells held at various potentials between –80 and +80 mV.

Voltage-jump records were obtained by bracketing a series of jumps in the presence of ACh with jumps done in the absence of agonist. Voltage-jump records were leak-subtracted averages of 12–18 jumps. Current relaxations were fit with a single exponential or the sum of two exponential components by using the BINFITS program. Best fits were determined by visual inspection.

Single-channel  $I$ – $V$  relationships were determined using voltage ramps and voltage jumps. An AI2020 event detector (Axon Instruments, Foster City, CA) was used to trigger the computer to initiate the voltage ramp or jump when a single

Table 1. Composition of intracellular solutions

Free Mg <sup>2+</sup> , μM	NaIse, mM	NaCl, mM	MgCl <sub>2</sub> , mM	Chelator, mM	Hepes, mM	pH
0	70	10	0	20 EDTA	40	7.3
300	110	9	0.5	10 EGTA	20	7.3
1000	110	6	2	10 EGTA	20	7.4
3000	110	0	5	10 EGTA	20	7.4

Values in the first column represent the calculated free Mg<sup>2+</sup> concentrations. The pH was titrated to the specified value with NaOH. Final Na<sup>+</sup> concentrations ranged from 148 to 152 mM. Nalse, sodium isethionate.

ACh-receptor channel opened. Single-channel records were leak-subtracted with traces taken in the absence of agonist. The *I-V* relationships determined using the voltage ramps were obtained by averaging traces in which the channel remained open for the entire ramp duration.

The extracellular bath contained 142 mM sodium isethionate, 2 mM NaCl, 1–2 mM MgCl<sub>2</sub>, and 20 mM Hepes (adjusted to pH 7.3 with NaOH), with osmolarity adjusted to 310 mosmol/kg by addition of glucose. Tetrodotoxin (1 μM) was added to the bath to block voltage-dependent Na<sup>+</sup> currents and isethionate was used to eliminate Cl<sup>-</sup> currents. In some experiments, atropine (500 nM) was added to the bath solution. Though atropine had no effect on outward currents, it had a voltage-dependent blocking effect on inward currents and therefore was not used in the experiments described in this paper. The standard intracellular pipette solution consisted of 130 mM sodium isethionate, 2 mM NaCl, 2 mM MgCl<sub>2</sub>, 20 mM Hepes, 10 mM EGTA-NaOH (adjusted to pH 7.3 with NaOH). For the experiments on Mg<sup>2+</sup> concentration dependence, the concentration of free Mg<sup>2+</sup> in the intracellular solutions (Table 1) was calculated using the stability constants for EDTA or EGTA (13).

ACh chloride was dissolved in bath solution and applied by local superfusion from a wide-tipped pipette (about 50 μm in diameter) positioned about 100 μm from the cell. The culture dish was continuously perfused with bath solution. All drugs

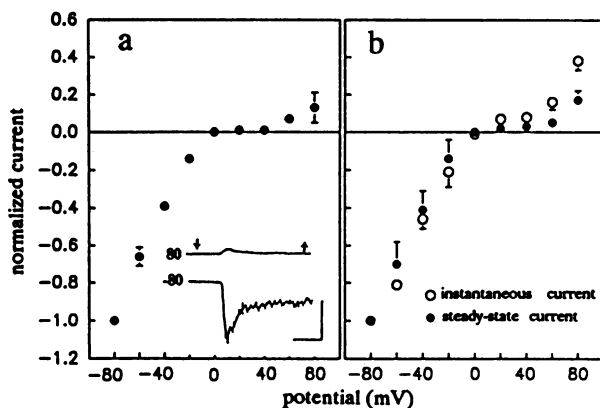


FIG. 1. *I-V* relationship of the peak whole-cell current. (a) PC12 cells were held at various potentials between -80 and +80 mV and superfused with 100 μM ACh. The peak current elicited by ACh at each potential was normalized to the current at -80 mV. Values are mean ± SD ( $n = 4$ ). (Inset) ACh-elicited currents at +80 and -80 mV are displayed. The perfuser was turned on at the downward arrow and off at the upward arrow. Horizontal scale bar, 500 msec; vertical bar, 500 pA. (b) Steady-state and instantaneous *I-V* relationships for the whole-cell ACh currents from voltage jumps. Currents were normalized to the current at -80 mV. For each jump, the instantaneous current was estimated to be the amplitude of the relaxation determined by extrapolation of the fitted curve to time zero. The baseline of the fitted exponential was taken to be the steady-state current. Values are mean ± SD of the normalized current ( $n = 3-6$  cells).

and compounds were obtained from Sigma unless specified otherwise.

## RESULTS

The whole-cell current response to an application of 100 μM ACh is characterized by a peak followed by a slow decline (Inset to Fig. 1a). The decline is most likely due to desensitization of the receptors. The activation processes of the receptors are in steady state during the response, but desensitization has not reached steady state during the time of agonist application. The *I-V* relationship for the peak whole-cell current elicited by ACh in PC12 cells is nonlinear (Fig. 1a). At negative potentials it curves downward, and at positive potentials it is flat between +10 and +40 mV then swings upward at potentials positive to +40 mV. The shape of the *I-V* curve remains unchanged whether the major intracellular cation is Na<sup>+</sup>, K<sup>+</sup>, or Cs<sup>+</sup> (C.K.I., unpublished data).

To determine the basis for the inward rectification of the whole-cell current, we examined the voltage dependence of the kinetics of whole-cell currents and the properties of currents through single channels.

**Current Relaxations After Voltage Jumps.** Voltage-jump experiments were done to estimate the voltage dependence of

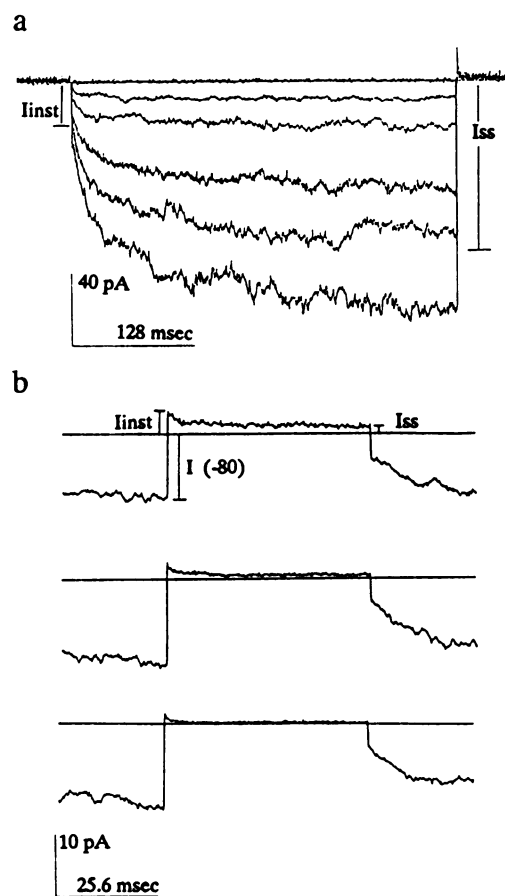


FIG. 2. Current relaxations after voltage jumps. Each current trace is the average of 5–10 consecutive jumps taken in the presence of 10 μM ACh. Capacitative and leak currents have been digitally subtracted using a control trace consisting of an average of 12–18 traces taken before and after ACh application. (a) Cell was held at +40 mV. Voltage steps, from bottom to top trace, were to -100, -80, -60, -40, -20, or 0 mV for 400 msec. (b) Voltage jumps, from the bottom trace to top, were to +40, +60, or +80 mV for 50 msec from a holding potential of -80 mV. *I*<sub>inst</sub>, instantaneous current; *I*<sub>ss</sub>, steady-state current.

channel gating. At low agonist concentrations, the time course of the current relaxation is an approximation for the channel burst duration (14). Two types of voltage-jump experiments were conducted: in the first set, cells were held at +40 mV and the voltage was stepped to negative potentials (-20, -40, -60, -80, and -100 mV; Fig. 2a), and in the second set, cells were held at -80 mV and the voltage steps were to positive potentials (40, 60, and 80 mV; Fig. 2b). The ACh concentration was 10  $\mu$ M, which is approximately an order of magnitude lower than that needed for half activation of the receptors as determined by flux measurements (15).

After stepping from +40 mV to a negative potential, a small instantaneous current,  $I_{inst}$ , was followed by an inward relaxation to a steady-state level,  $I_{ss}$  (Fig. 2a). The instantaneous current increased linearly with test potential (Fig. 1b), consistent with a constant single-channel conductance for inward current. The time course of the current relaxations could be described by the sum of two exponential components. At -80 mV, the faster time constant ( $\tau_1$ ) was  $10 \pm 5$

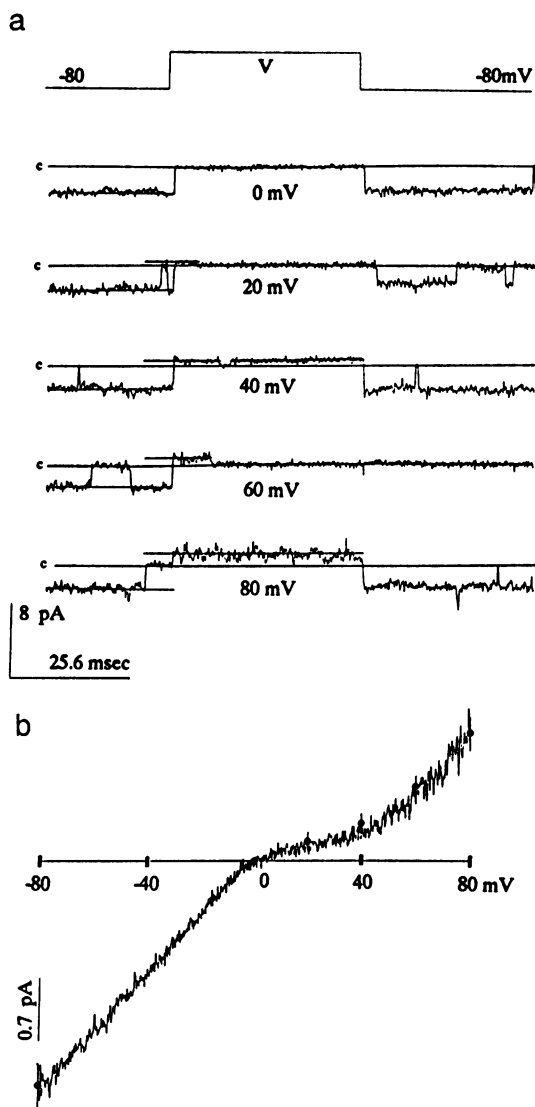


FIG. 3. Single-channel  $I$ - $V$  relationship. Outside-out patches were held at -80 mV and exposed to 10  $\mu$ M ACh. (a) The voltage across the patch was stepped to 0, +20, +40, +60, or +80 mV after a channel remained open for 35 msec. Channels are closed at the lines labeled "c." (b) The single-channel currents from the voltage jumps (solid circles; mean  $\pm$  SD,  $n = 10$ -20) are superimposed upon the single-channel  $I$ - $V$  relationship determined using voltage ramps. Ramps went from -80 mV to +80 mV in 100 msec. The current trace is the leak-subtracted average of 15 ramps.

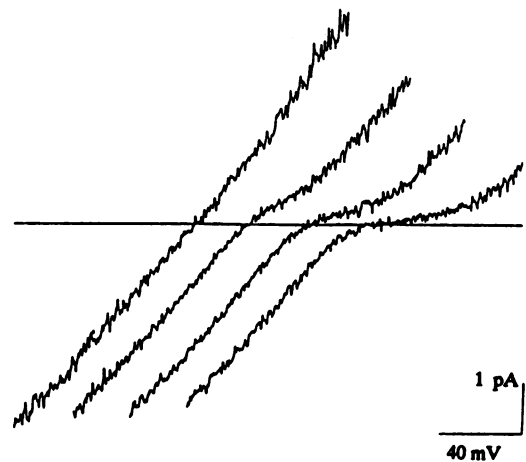


FIG. 4. Single-channel  $I$ - $V$  relationship with different concentrations of intracellular  $Mg^{2+}$ . From left to right, the intracellular free  $Mg^{2+}$  concentrations were 0, 0.3, 1, and 3 mM. The current traces have been offset in relation to one another; all currents reversed close to 0 mV. The applied voltage ramps increased linearly from -80 (left) to +80 mV (right) in 25 msec. Each trace is the average of 13-19 leak-subtracted current traces.

msec and the slow one ( $\tau_2$ ),  $78 \pm 6$  msec ( $n = 6$ ). PC12 cells express at least two nicotinic ACh receptors distinguished by differences in conductance (16) and open time (C.K.I., unpublished data). The larger-conductance channel is more prevalent in outside-out patches (>90% of the openings) and has burst duration close in value to  $\tau_2$ .  $\tau_2$ , evaluated at potentials between -20 mV and -100 mV, increased  $e$ -fold over -123 mV (data not shown).

Current relaxations resulting from jumps from -80 mV to positive potentials were small (Fig. 2b) and the  $I_{inst}$ - $V$  relationship for these jumps was not ohmic (Fig. 1b). This is most easily seen for the voltage jump from -80 to +80 mV. The inward current at -80 mV before the voltage jump is  $\approx 10$  pA. The instantaneous outward current at +80 mV is only 2 pA, although the magnitude of the electrochemical potential across the membrane for  $Na^+$  is the same at -80 mV and +80 mV and the same number of channels should be open immediately before and after the jump. A nonlinear  $I_{inst}$ - $V$  curve is not consistent with an ohmic single-channel  $I$ - $V$  relationship. The current relaxations were fitted with a single exponential with time constants ranging from 2 to 5 msec. The time constants did not have a clear voltage dependence. Extrapolating from the values of  $\tau_2$  in the negative potential range, a time constant of about 25-30 msec was expected at +40 mV. However, the small size of the outward current relaxation may have made this component of the relaxation difficult to detect.

**Single-Channel  $I$ - $V$  Relationship.** The single-channel  $I$ - $V$  relation for the larger-conductance channel was determined using voltage jumps (Fig. 3a) and voltage ramps (Fig. 3b). The  $I$ - $V$  relation for this channel is linear at negative potentials and the slope conductance for the inward current is 32 pS. The  $I$ - $V$  relation is nonlinear positive to 0 mV. The outward single-channel conductance is reduced compared to the inward conductance so that at +20 mV, the chord conductance is only about 8 pS. Positive to +40 mV, the single-channel conductance increases.

The inward rectification of the single ACh-receptor channel is strongly dependent on the intracellular  $Mg^{2+}$  concentration (Fig. 4). The single-channel  $I$ - $V$  curve in Fig. 3 was obtained using the standard intracellular solution, which has a free  $Mg^{2+}$  concentration of 1.3 mM. Decreasing the intracellular  $Mg^{2+}$  concentration to 0 linearizes the single-channel  $I$ - $V$  relationship; the slope conductance is 49 pS. An increase in the intracellular  $Mg^{2+}$  concentration results in a reduction

of the outward current through the channel. With 3 mM intracellular  $Mg^{2+}$ , the outward chord conductance at +20 mV is diminished to 4 pS. The  $EC_{50}$  for the reduction of outward current measured at +20 mV is  $\approx 200 \mu M$ . The blocking effect of  $Mg^{2+}$  is asymmetrical, since with 1 mM  $Mg^{2+}$  in the extracellular bath and 0  $Mg^{2+}$  on the intracellular side, the single-channel  $I-V$  relationship is linear. Intracellular  $Mg^{2+}$  also appears to have a small effect on inward currents; the inward conductance decreases from 49 pS with 0  $Mg^{2+}$  to 45 pS with 3 mM intracellular  $Mg^{2+}$ . The larger single-channel currents for the data in Fig. 4 are due to the fact that these experiments were conducted at a higher temperature (25°C vs. 18°C). To date, we have tested the blocking effects of internal  $Mg^{2+}$  only, as it appeared to be the most physiologically relevant divalent cation.

## DISCUSSION

Two voltage-dependent processes appear to mediate the rectification of the macroscopic ACh current in PC12 cells: (i) the voltage-dependence of the channel mean burst duration and (ii) ion permeation through the single ACh-receptor channel. The voltage dependence of the channel burst duration shapes the  $I-V$  relation of the inward whole-cell current. Dependent on the burst duration, the inward  $I-V$  relationship is established relatively slowly. In contrast, the  $I-V$  relationship of the outward current is established quickly since the block by intracellular  $Mg^{2+}$  ions is rapid. Such a rapid block would be manifest during the short duration of a postsynaptic potential and could explain the reduction of peak postsynaptic current amplitudes at positive potentials as seen in mouse submandibular ganglion cells (2) and rabbit SCG cells (1).

The channel burst duration of the PC12 ACh receptor shows a voltage dependence similar to those estimated from ACh current noise in rat adrenal chromaffin cells (burst duration of 76 msec at -100 mV increasing  $e$ -fold over -137 mV; ref. 5). Burst durations for receptors on mouse submandibular ganglion cells (2) and rat SCG cells (6) are more sensitive to voltage, increasing  $e$ -fold over -46 and -70 mV, respectively.

The single-channel  $I-V$  relationship for the larger-conductance PC12 ACh receptor is linear at negative potentials, with a slope conductance of about 32 pS at 18°C. This value is in the range of those found for other rat ganglionic nicotinic receptors (20–50 pS; refs. 2, 3, 17, and 18). At positive potentials, the single-channel  $I-V$  is nonlinear when the intracellular  $Mg^{2+}$  concentration is  $>50 \mu M$ . Between 0 and +40 mV, the conductance is reduced compared to the single-channel conductance for inward currents. Positive to +40 mV, there is an increase in single-channel conductance that can explain the upturn in the whole-cell  $I-V$  relationship seen at these potentials.

From the voltage dependence of the channel burst duration and the single-channel  $I-V$  relationship, major features of the whole-cell  $I-V$  relationship can be predicted. In doing so, we make the following assumptions. First, the population of nicotinic ACh receptors is functionally homogeneous. Although PC12 cells express at least two different kinds of receptors, the contribution of the larger-conductance channel probably dominates the whole-cell current since in addition to its larger conductance, it is more prevalent and has a substantially longer burst duration. Second, the number of activatable receptors remains constant. The normalized ACh-induced current can then be expressed as

$$I(v)/I(-80) = [i(v)/i(-80)] \times [P_o(v)/P_o(-80)],$$

where  $i(v)$  is the single-channel current as a function of voltage, and  $P_o(v)$  is the probability that the channel is open.

Under a third assumption that the channel opening rate is small and relatively voltage independent, the ratio of open probabilities,  $P_o(v)/P_o(-80)$  can be approximated by  $\tau(v)/\tau(-80)$ , the ratio of the channel burst duration. This gives us the following equation for the normalized current:

$$I(v)/I(-80) = [i(v)/i(-80)] \times [\tau(v)/\tau(-80)].$$

The predicted  $I-V$  relationship (Fig. 5, dotted line) can account for many of the features of the whole-cell  $I-V$  relation. At potentials negative to 0, the downward curvature results from the increase in channel burst duration with hyperpolarization. At positive potentials, the predicted  $I-V$  relation is dominated by the shape of the single-channel  $I-V$  relationship. However, between +20 and +40 mV, the predicted  $I-V$  curve lies above the plot of the experimentally derived whole-cell  $I-V$  relationship. This may indicate that some of our assumptions do not hold and another process is involved in the rectification of the whole-cell current (e.g., voltage dependence of channel opening). Alternatively, neglecting the second class of channels may underlie the mismatch at these potentials.

Mathie *et al.* (3) observed that the strong inward rectification of whole-cell ACh-elicited currents in rat SCG cells remained whether or not divalent cations were present. Although recent experiments on nicotinic receptors of rat SCG cells have revealed that these receptors are also blocked by internal  $Mg^{2+}$  (19), the question remains why the removal of divalent ions from the extracellular and intracellular solutions failed to linearize the whole-cell  $I-V$  relationship. In PC12 cells as well, attempts to remove intracellular  $Mg^{2+}$  only partially relieve the rectification of the whole-cell currents. Possible explanations include failure to completely remove divalent cations from the vicinity of the receptors, or presence of an additional blocking mechanism in perfused cells.

The single-channel rectification of the PC12 cell ACh-receptor channel results from a voltage-dependent reduction of outward current produced by cytoplasmic  $Mg^{2+}$  ions. Voltage-dependent block of outward currents by intracellular  $Mg^{2+}$  has been described for several cation channels, notably inwardly rectifying  $K^+$  channels (20, 21). Extracellular  $Mg^{2+}$  ions can also block inward currents, for example the *N*-methyl-D-aspartate (NMDA)-receptor channel (22, 23). Both the inwardly rectifying  $K^+$  channel and the NMDA-receptor channel are more sensitive to block by  $Mg^{2+}$  than the PC12

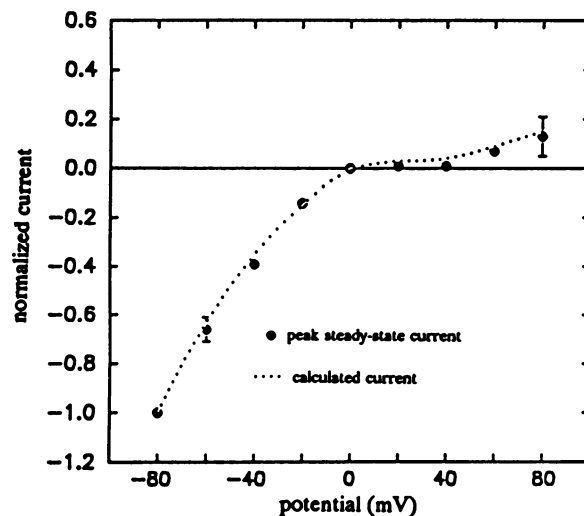


FIG. 5. Predicted and experimentally derived  $I-V$  relationships. The predicted  $I-V$  relation (dotted line; see text) is compared to the observed peak whole-cell  $I-V$  relation (●; see Fig. 1).

ACh-receptor channel: the inward rectifier is half-blocked by  $1.7 \mu\text{M Mg}^{2+}$  at  $+70 \text{ mV}$  (24), whereas the NMDA-receptor channel has a  $K_D$  of  $72 \mu\text{M}$  for  $\text{Mg}^{2+}$  at  $-60 \text{ mV}$  (25). In comparison, the PC12 ACh-receptor channel is half-blocked by  $200 \mu\text{M Mg}^{2+}$  at  $+20 \text{ mV}$ .

The properties of the block of the PC12 ACh-receptor channel by  $\text{Mg}^{2+}$  can give some insight into the qualitative features of the open channel. Assuming that a one-site, two-barrier model is appropriate for the channel (26), we draw the following conclusions. The increase in conductance at potentials positive to  $+40 \text{ mV}$  suggests that the inhibitory effect of  $\text{Mg}^{2+}$  on outward currents is not due to charge screening at the vestibule of the channel. The upturn of the single-channel  $I-V$  relationship may reflect relief of block as  $\text{Mg}^{2+}$  is forced out of the binding site within the channel at the higher membrane potentials. The low concentrations of  $\text{Mg}^{2+}$  needed to block outward currents suggest that the binding site within the channel has a higher affinity for  $\text{Mg}^{2+}$  than for  $\text{Na}^+$ , as found for muscle nicotinic ACh receptors. Finally, the asymmetry of the  $\text{Mg}^{2+}$  block suggests that the inner energy barrier (on the cytoplasmic side) is lower for  $\text{Mg}^{2+}$  than the outer one.

A physiological role for the rectification of the nicotinic receptor currents has not been demonstrated. While the nonlinear  $I-V$  relationship for ACh-receptor currents appears to be a characteristic feature of peripheral neuronal nicotinic ACh receptors, the whole-cell ACh-elicited  $I-V$  relationship is linear for rat retinal ganglion cells (27). PC12 cells express the mRNA for at least two  $\alpha$  and two  $\beta$  neuronal nicotinic receptor subunits (28–31). Several combinations of these subunits have been expressed in *Xenopus* oocytes and none appears to correspond to the dominant receptor type seen in PC12 cells (31). Considering the functional differences between the neuronal nicotinic receptors examined so far, some insight into the relationship between receptor structure and function will be gained as more functional information becomes available for receptors with known structures.

We wish to thank C. Kopta, C. Lingle, J. Nerbonne, M. Takenoshita, and J. Zempel for discussions and for critical reading of the manuscript. This work was supported by Grant R01 NS22356 from the National Institutes of Health (J.H.S.) and Training Grant 2T32 HL07275-11 from the U.S. Department of Health and Human Services (C.K.I.).

1. Derkach, V. A., Selyanko, A. A. & Skok, V. I. (1983) *J. Physiol. (London)* **336**, 511–526.
2. Yawo, H. (1989) *J. Physiol. (London)* **417**, 307–322.
3. Mathie, A., Cull-Candy, S. G. & Colquhoun, D. (1987) *Proc. R. Soc. Lond. Ser. B* **232**, 239–248.
4. Colquhoun, D., Cull-Candy, S. G. & Mathie, A. (1989) *J. Physiol. (London)* **410**, 28P (abstr).
5. Hirano, T., Kidokoro, Y. & Ohmori, H. (1987) *Pflügers Arch.* **408**, 401–407.
6. Selyanko, A. A., Derkach, V. A. & Kurennyi, D. E. (1988) *Neurophysiology* **20**, 122–126.
7. Greene, L. A. & Tischler, A. S. (1976) *Proc. Natl. Acad. Sci. USA* **73**, 2424–2428.
8. Dichter, M. A., Tischler, A. S. & Greene, L. A. (1977) *Nature (London)* **268**, 501–504.
9. Patrick, J. & Stallcup, W. B. (1977) *Proc. Natl. Acad. Sci. USA* **74**, 4689–4692.
10. Patrick, J. & Stallcup, B. (1977) *J. Biol. Chem.* **252**, 8629–8633.
11. Ifune, C. K. & Steinbach, J. H. (1990) *Brain Res.* **560**, 243–248.
12. Hamill, O., Marty, A., Neher, E., Sakmann, B. & Sigworth, F. (1981) *Pflügers Arch.* **391**, 85–100.
13. Martell, A. E. & Smith, R. M. (1974) in *Critical Stability Constants* (Plenum, New York), Vol. 1, pp. 204–272.
14. Neher, E. & Sakmann, B. (1975) *Proc. Natl. Acad. Sci. USA* **72**, 2140–2144.
15. Boyd, N. (1987) *J. Physiol. (London)* **389**, 45–67.
16. Bormann, J. & Mattheaei, H. (1983) *Neurosci. Lett.* **40**, 193–197.
17. Adams, D. J., Fieber, L. A. & Konishi, S. (1987) *J. Physiol. (London)* **394**, 153P (abstr.).
18. Derkach, V. A., North, R. A., Selyanko, A. A. & Skok, V. I. (1987) *J. Physiol. (London)* **388**, 141–151.
19. Mathie, A., Colquhoun, D. & Cull-Candy, S. G. (1990) *J. Physiol.*, in press.
20. Matsuda, H., Saigusa, A. & Irisawa, H. (1987) *Nature (London)* **325**, 156–159.
21. Vandenberg, C. A. (1987) *Proc. Natl. Acad. Sci. USA* **84**, 2560–2564.
22. Nowak, L., Bregestovski, P., Ascher, P., Herbet, A. & Prochiantz, A. (1984) *Nature (London)* **307**, 462–465.
23. Mayer, M. L., Westbrook, G. L. & Guthrie, P. B. (1984) *Nature (London)* **309**, 261–263.
24. Matsuda, H. (1988) *J. Physiol.* **397**, 237–258.
25. Ascher, P. & Nowak, L. (1988) *J. Physiol.* **399**, 247–266.
26. Dani, J. A. & Eisenman, G. (1987) *J. Gen. Physiol.* **89**, 959–983.
27. Lipton, S. A., Aizenmann, E. & Loring, R. H. (1987) *Pflügers Arch.* **410**, 37–43.
28. Boulter, J., Evans, K., Goldman, D., Matin, G., Treco, D., Heinemann, S. & Patrick, J. (1986) *Nature (London)* **319**, 368–374.
29. Deneris, E. S., Connolly, J., Boulter, J., Wada, E., Wada, K., Swanson, L. W., Patrick, J. & Heinemann, S. (1988) *Neuron* **1**, 45–54.
30. Duvoisin, R. M., Deneris, E. S., Patrick, J. & Heinemann, S. (1989) *Neuron* **3**, 487–496.
31. Papke, R. L. (1989) *Neuron* **3**, 589–596.